

# Using non-DESI data to confirm and strengthen the DESI 2024 spatially-flat $w_0w_a$ CDM cosmological parameterization result

Chan-Gyung Park \*

*Division of Science Education and Institute of Fusion Science,  
Jeonbuk National University, Jeonju 54896, Republic of Korea*

Javier de Cruz Pérez †

*Departamento de Física Teórica, Universidad Complutense de Madrid, 28040, Madrid, Spain*

Bharat Ratra ‡

*Department of Physics, Kansas State University, 116 Cardwell Hall, Manhattan, KS 66506, USA*  
(Dated: May 2, 2024)

We use a combination of Planck cosmic microwave background (CMB) anisotropy data and non-CMB data that include Pantheon+ type Ia supernovae, Hubble parameter [ $H(z)$ ], growth factor ( $f\sigma_8$ ) measurements, and a collection of baryon acoustic oscillation (BAO) data, but not recent DESI 2024 BAO measurements, to confirm the DESI 2024 (DESI+CMB+PantheonPlus) data compilation support for dynamical dark energy with an evolving equation of state parameter  $w(z) = w_0 + w_a z/(1+z)$ . From our joint compilation of CMB and non-CMB data, in a spatially-flat cosmological model, we obtain  $w_0 = -0.850 \pm 0.059$  and  $w_a = -0.59^{+0.26}_{-0.22}$  and find that this dynamical dark energy is favored over a cosmological constant by  $\sim 2\sigma$ . Our data constraints on the flat  $w_0w_a$ CDM model are slightly more restrictive than the DESI 2024 constraints, with the DESI 2024 and our values of  $w_0$  and  $w_a$  differing by  $-0.27\sigma$  and  $0.44\sigma$ , respectively. Our data compilation slightly more strongly favors the flat  $w_0w_a$ CDM model over the flat  $\Lambda$ CDM model than does the DESI 2024 data compilation.

PACS numbers: 98.80.-k, 95.36.+x

## I. INTRODUCTION

In the six-parameter spatially-flat  $\Lambda$ CDM cosmological model, [1], the observed currently accelerated cosmological expansion is a general-relativistic gravitational effect sourced by the cosmological constant  $\Lambda$  that currently dominates the cosmological energy budget with pressureless cold dark matter (CDM) being the next largest contributor to the current energy budget. While the currently-standard spatially-flat  $\Lambda$ CDM model is generally consistent with most observational constraints, some current measurements might be incompatible with the predictions of this model, [2–5].

Recent DESI baryon acoustic oscillation (BAO) measurements, [6], might be incompatible with the predictions of the standard flat  $\Lambda$ CDM model. In an analysis of the spatially-flat  $w_0w_a$ CDM cosmological parameterization where dynamical dark energy is modelled as a fluid with an evolving equation of state parameter  $w(z) = w_0 + w_a z/(1+z)$ , [7, 8], DESI+CMB+PantheonPlus data (described below) favor  $w_0 = -0.827 \pm 0.063$  and  $w_a = -0.75^{+0.29}_{-0.25}$ , approximately  $2\sigma$  away from the cosmological constant point at  $w_0 = -1$  and  $w_a = 0$ . (We note that in the following we use  $w_0$  and  $w$  interchange-

ably.) For other discussions of constraints on dynamical dark energy see [9–19] and references therein.

Here we use the P18+lensing+non-CMB data set of [19], where non-CMB data includes Pantheon+ SNIa data, and in particular BAO data that does not include the recent DESI 2024 BAO measurements. We confirm the DESI 2024 support for dynamical dark energy with an evolving equation of state parameter  $w(z) = w_0 + w_a z/(1+z)$ , but now with  $w_0 = -0.850 \pm 0.059$  and  $w_a = -0.59^{+0.26}_{-0.22}$ , which suggests that dynamical dark energy is preferred over a cosmological constant by  $\sim 2\sigma$ . Our P18+lensing+non-CMB data constraints on the flat  $w_0w_a$ CDM model are slightly more restrictive than those derived in [6], while also slightly more strongly favoring the flat  $w_0w_a$ CDM model over the flat  $\Lambda$ CDM model than found in [6].

While interesting, these results are not statistically significant. More importantly  $w(z) = w_0 + w_a z/(1+z)$  is a parameterization and not a physically consistent dynamical dark energy model. The simplest physically-consistent dynamical dark energy models use a dynamical scalar field  $\phi$  with a self-interaction potential energy density  $V(\phi)$  as dynamical dark energy, [20, 21]. For recent discussions of dynamical scalar field dark energy models in the context of DESI 2024 measurements, see [22–24]. For other discussions of the DESI 2024 results, see [25–30].

In Sec. II we provide brief details of the data sets we use to constrain cosmological parameters in, and test the performance of, the flat  $w_0w_a$ CDM model. In Sec. III we

\* park.chan.gyung@gmail.com

† jadecruz@ucm.es

‡ ratra@phys.ksu.edu

briefly summarize the main features of the flat  $w_0w_a$ CDM model and the analysis techniques we use. Our results are presented and discussed in Sec. IV, and we conclude in Sec. V.

## II. DATA

In this work CMB and non-CMB data sets are used to constrain the parameters of a dynamical dark energy model. The data sets we use in our analyses here are described in detail in Sec. II of [19] and outlined in what follows. We account for all known data covariances.

For the CMB data, we use the Planck 2018 TT,TE,EE+lowE (P18) CMB temperature and polarization power spectra alone as well as jointly with the Planck lensing potential (lensing) power spectrum [31, 32].

The non-CMB data set we use is the non-CMB (new) data compilation of [19], which is comprised of

- 16 BAO data points, spanning  $0.122 \leq z \leq 2.334$ , listed in Table I of [19]. We do not use DESI 2024 BAO data, [6].
- A 1590 SNIa data point subset of the Pantheon+ compilation [33], retaining only SNIa with  $z > 0.01$  to mitigate peculiar velocity correction effects. These data span  $0.01016 \leq z \leq 2.26137$ ,
- 32 Hubble parameter [ $H(z)$ ] measurements, spanning  $0.070 \leq z \leq 1.965$ , listed in Table 1 of [34] and in Table II of [19].
- An additional nine (non-BAO) growth rate ( $f\sigma_8$ ) data points, spanning  $0.013 \leq z \leq 1.36$ , listed in Table III of [19].

We use five individual and combined data sets to constrain the flat  $w_0w_a$ CDM and flat  $\Lambda$ CDM models: P18 data, P18+lensing data, non-CMB data, P18+non-CMB data, and P18+lensing+non-CMB data.

## III. METHODS

The methods we use are described in Sec. III of [19]. A brief summary follows.

To determine quantitatively how tightly these observational data constrain the cosmological model parameters, we use the CAMB/COSMOMC program (October 2018 version) [35–37]. CAMB computes the evolution of model spatial inhomogeneities and makes theoretical predictions which depend on cosmological parameters while COSMOMC compares these predictions to observational data, using the Markov chain Monte Carlo (MCMC) method, to determine cosmological parameter likelihoods. The MCMC chains are assumed to have converged when the Gelman and Rubin  $R$  statistic satisfies  $R - 1 < 0.01$ . For each model and data set, we use the converged MCMC chains,

with the `GetDist` code [38], to compute the average values, confidence intervals, and likelihood distributions of model parameters.

In the flat  $\Lambda$ CDM model, the six primary cosmological parameters are conventionally chosen to be the current value of the physical baryonic matter density parameter  $\Omega_b h^2$ , the current value of the physical cold dark matter density parameter  $\Omega_c h^2$ , the angular size of the sound horizon at recombination  $100\theta_{\text{MC}}$ , the reionization optical depth  $\tau$ , the primordial scalar-type perturbation power spectral index  $n_s$ , and the power spectrum amplitude  $\ln(10^{10} A_s)$ , where  $h$  is the Hubble constant in units of  $100 \text{ km s}^{-1} \text{ Mpc}^{-1}$ . We assume flat priors for these parameters, non-zero over:  $0.005 \leq \Omega_b h^2 \leq 0.1$ ,  $0.001 \leq \Omega_c h^2 \leq 0.99$ ,  $0.5 \leq 100\theta_{\text{MC}} \leq 10$ ,  $0.01 \leq \tau \leq 0.8$ ,  $0.8 \leq n_s \leq 1.2$ , and  $1.61 \leq \ln(10^{10} A_s) \leq 3.91$ . In the  $w_0w_a$ CDM model dynamical dark energy is assumed to be a fluid with an evolving equation of state parameter (fluid pressure to energy density ratio)  $w(z) = w_0 + w_a z / (1+z)$ , [7, 8], and for the additional dark energy equation of state parameters we also adopt flat priors non-zero over  $-3.0 \leq w_0 \leq 0.2$  and  $-3 < w_a < 2$ . When we estimate parameters using non-CMB data, we fix the values of  $\tau$  and  $n_s$  to those obtained from P18 data (since these parameters cannot be determined solely from non-CMB data) and constrain the other cosmological parameters. Additionally, we also present constraints on three derived parameters, namely the Hubble constant  $H_0$ , the current value of the non-relativistic matter density parameter  $\Omega_m$ , and the amplitude of matter fluctuations  $\sigma_8$ , which are obtained from the primary parameters of the cosmological model.

For the flat tilted  $w_0w_a$ CDM model the primordial scalar-type energy density perturbation power spectrum is

$$P_\delta(k) = A_s \left( \frac{k}{k_0} \right)^{n_s}, \quad (1)$$

where  $k$  is the wavenumber and  $n_s$  and  $A_s$  are the spectral index and the amplitude of the spectrum at pivot scale  $k_0 = 0.05 \text{ Mpc}^{-1}$ . This power spectrum is generated by quantum fluctuations during an early epoch of power-law inflation in a spatially-flat inflation model powered by a scalar field inflaton potential energy density that is an exponential function of the inflaton [39–41].

To quantify how relatively well each model fits the data set under study, we use the differences in the Akaike information criterion ( $\Delta\text{AIC}$ ) and the deviance information criterion ( $\Delta\text{DIC}$ ) between the information criterion (IC) values for the flat  $w_0w_a$ CDM model and the flat  $\Lambda$ CDM model. See Sec. III of [19] for a fuller discussion. According to the Jeffreys' scale, when  $-2 \leq \Delta\text{IC} < 0$  there is *weak* evidence in favor of the model under study, while when  $-6 \leq \Delta\text{IC} < -2$  there is *positive* evidence, when  $-10 \leq \Delta\text{IC} < -6$  there is *strong* evidence, and when  $\Delta\text{IC} < -10$  there is *very strong* evidence in favor of the model under study relative to the tilted flat  $\Lambda$ CDM model. This scale also holds when  $\Delta\text{IC}$  is posi-

TABLE I. Mean and 68% (or 95%) confidence limits of flat  $w_0w_a$ CDM model parameters from non-CMB, P18, P18+lensing, P18+non-CMB, and P18+lensing+non-CMB data.  $H_0$  has units of  $\text{km s}^{-1} \text{Mpc}^{-1}$ .

Parameter	Non-CMB	P18	P18+lensing	P18+non-CMB	P18+lensing+non-CMB
$\Omega_b h^2$	$0.315 \pm 0.0043$	$0.02240 \pm 0.00015$	$0.02243 \pm 0.00015$	$0.02245 \pm 0.00014$	$0.02244 \pm 0.00014$
$\Omega_c h^2$	$0.0990^{+0.0061}_{-0.011}$	$0.1199 \pm 0.0014$	$0.1192 \pm 0.0012$	$0.1190 \pm 0.0011$	$0.1191 \pm 0.0010$
$100\theta_{\text{MC}}$	$1.0218^{+0.0087}_{-0.011}$	$1.04094 \pm 0.00031$	$1.04101 \pm 0.00031$	$1.04101 \pm 0.00030$	$1.04100 \pm 0.00029$
$\tau$	0.0540	$0.0540 \pm 0.0079$	$0.0523 \pm 0.0074$	$0.0529 \pm 0.0077$	$0.0534 \pm 0.0072$
$n_s$	0.9654	$0.9654 \pm 0.0043$	$0.9669 \pm 0.0041$	$0.9672 \pm 0.0040$	$0.9670 \pm 0.0039$
$\ln(10^{10} A_s)$	$3.60 \pm 0.24 (> 3.13)$	$3.043 \pm 0.016$	$3.038 \pm 0.014$	$3.039 \pm 0.016$	$3.040 \pm 0.014$
$w$	$-0.876 \pm 0.055$	$-1.25^{+0.43}_{-0.56}$	$-1.24^{+0.44}_{-0.56}$	$-0.853 \pm 0.061$	$-0.850 \pm 0.059$
$w_a$	$0.10^{+0.32}_{-0.20}$	$-1.3 \pm 1.2 (< 1.13)$	$-1.2 \pm 1.3 (< 1.19)$	$-0.57^{+0.27}_{-0.23}$	$-0.59^{+0.26}_{-0.22}$
$H_0$	$69.8 \pm 2.4$	$84 \pm 11 (> 64.5)$	$84 \pm 11 (> 64.7)$	$67.81 \pm 0.64$	$67.80 \pm 0.64$
$\Omega_m$	$0.2692^{+0.0086}_{-0.015}$	$0.213^{+0.016}_{-0.070}$	$0.213^{+0.017}_{-0.071}$	$0.3092 \pm 0.0063$	$0.3094 \pm 0.0063$
$\sigma_8$	$0.823^{+0.031}_{-0.027}$	$0.955^{+0.11}_{-0.050}$	$0.945^{+0.11}_{-0.048}$	$0.810 \pm 0.011$	$0.8108 \pm 0.0091$
$\chi^2_{\text{min}}$	1457.16	2761.18	2770.39	4234.18	4243.01
$\Delta\chi^2_{\text{min}}$	-12.77	-4.62	-4.32	-6.06	-6.25
DIC	1470.93	2815.45	2824.19	4290.48	4298.75
$\Delta$ DIC	-7.18	-2.48	-2.26	-1.85	-2.45
AIC	1469.16	2819.18	2828.39	4292.18	4301.01
$\Delta$ AIC	-8.77	-0.62	-0.32	-2.05	-2.25

tive, but then the tilted flat  $\Lambda$ CDM model is favored over the model under study.

To quantitatively compare how consistent the cosmological parameter constraints (for the same model) derived from two different data sets are, we use two estimators. The first is the DIC based  $\log_{10} \mathcal{I}$ , see [42] and Sec. III of [19]. When the two data sets are consistent  $\log_{10} \mathcal{I} > 0$  while  $\log_{10} \mathcal{I} < 0$  means that the two data sets are inconsistent. According to the Jeffreys' scale the degree of consistency or inconsistency between two data sets is *substantial* if  $|\log_{10} \mathcal{I}| > 0.5$ , *strong* if  $|\log_{10} \mathcal{I}| > 1$ , and *decisive* if  $|\log_{10} \mathcal{I}| > 2$ , [42]. The second estimator is the tension probability  $p$  and the related, Gaussian approximation, "sigma value"  $\sigma$ , see [43–45] and Sec. III of [19].  $p = 0.05$  and  $p = 0.003$  correspond to  $2\sigma$  and  $3\sigma$  Gaussian standard deviation.

#### IV. RESULTS AND DISCUSSION

Cosmological parameter constraints are listed in Table I and shown in Figs. 1 and 2, with just the  $w_0 - w_a$  panels of these figures reproduced in Figs. 3. Values of the statistical estimators used to assess consistency between P18 and non-CMB data cosmological constraint results and between P18+lensing and non-CMB data results are listed in Table II, while  $\Delta\chi^2_{\text{min}}$ ,  $\Delta$ AIC, and  $\Delta$ DIC values

are listed in Table I.

From Table I and Figs. 1 and 2 we see that non-CMB data provide significantly more restrictive constraints on  $w$  and  $w_a$ , as well as on derived parameters  $H_0$ ,  $\Omega_m$ , and  $\sigma_8$ , than do P18 or P18+lensing data. This is very similar to what happens in the XCDM (or  $w$ CDM) model, to which the  $w_0w_a$ CDM model studied here reduces when  $w_a = 0$ , see the discussion in Sec. IV.B of [19].

Table II shows that non-CMB and P18+lensing data constraints are incompatible at  $2.7\sigma$  in the flat  $w_0w_a$ CDM model (with non-CMB and P18 data being slightly more incompatible at  $2.8\sigma$ ) according to the second ( $p$  and  $\sigma$ ) estimator we use; according to  $\log_{10} \mathcal{I}$  there is a substantial tension between the two data sets. This should be compared to the  $1.2\sigma$  compatibility and  $3.6\sigma$  incompatibility between these two data sets in the flat  $\Lambda$ CDM model and the flat XCDM model, respectively, see Tables X and XIV of [19], where according to  $\log_{10} \mathcal{I}$  there is substantial consistency (flat  $\Lambda$ CDM) and decisive inconsistency (flat XCDM) between these data sets. One may conclude that these data rule out the flat  $w_0w_a$ CDM model at  $2.7\sigma$  (or  $2.8\sigma$ ), but given the current state of the field we instead conclude that P18 or P18+lensing data and non-CMB data are compatible at better than  $3\sigma$  in the flat  $w_0w_a$ CDM model and so can be jointly used to constrain cosmological parameters in this model. In the following discussion we will focus more on the P18+lensing+non-CMB data results, as that is the

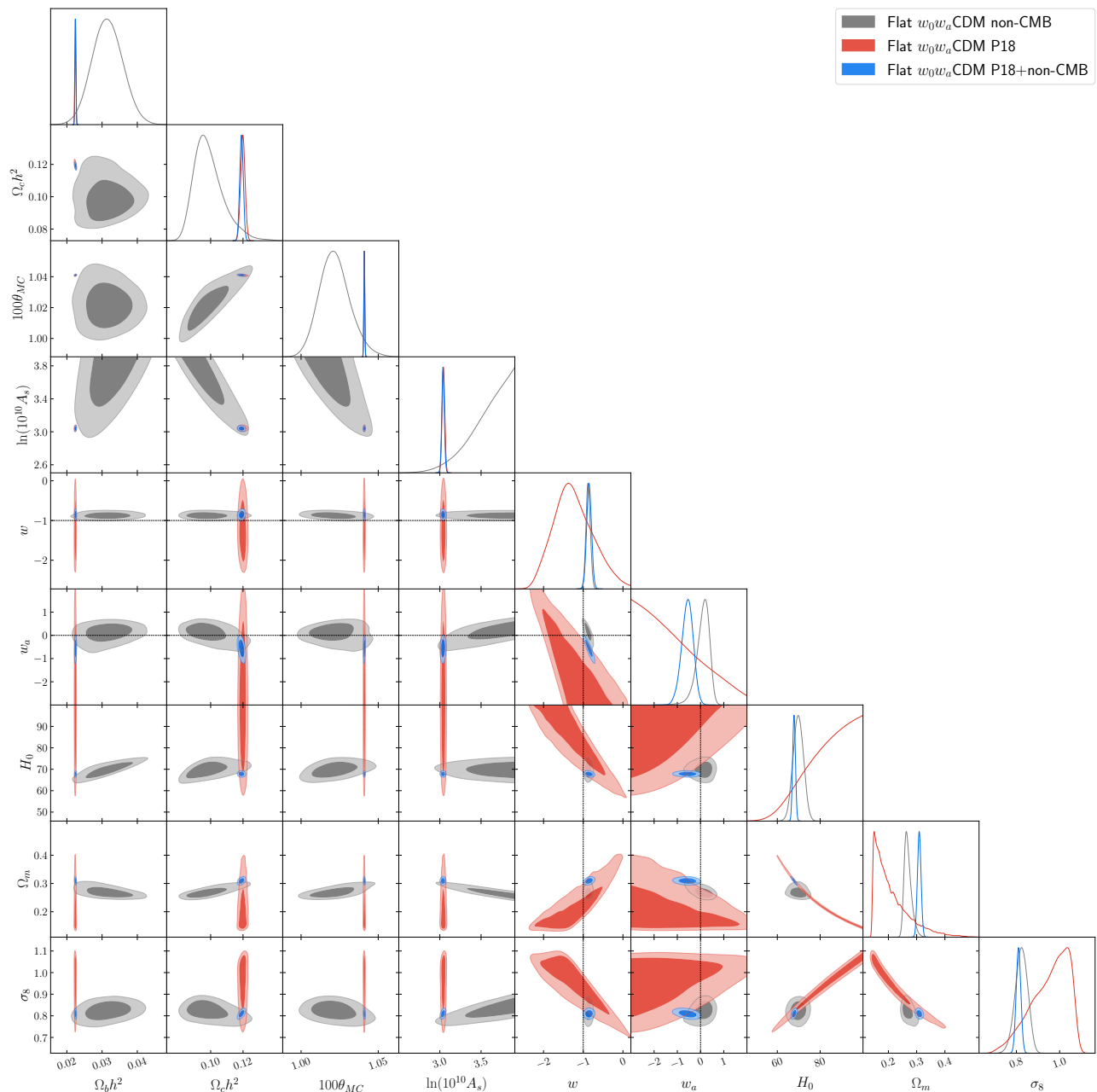


FIG. 1. One-dimensional likelihoods and  $1\sigma$  and  $2\sigma$  likelihood confidence contours of flat  $w_0w_a$ CDM model parameters favored by non-CMB, P18, and P18+non-CMB data sets. We do not show  $\tau$  and  $n_s$ , which are fixed in the non-CMB data analysis.

largest data set we use.

In an attempt to better support our choice to somewhat downplay the  $2.7\sigma$  and  $2.8\sigma$  incompatibilities discussed in the previous paragraph, we note that in addition to the flat  $\Lambda$ CDM model issues alluded to in Sec. I there are two less widely discussed puzzles with some of the data sets we use. One has to do with P18 data in the seven-parameter flat  $\Lambda$ CDM+ $A_L$  model where the phenomenological lensing consistency parameter  $A_L$  is introduced to rescale the amplitude of the gravitational potential power spectrum, [46]. Here  $A_L = 1$  corre-

sponds to the theoretically predicted (using the best-fit cosmological parameter values) amount of weak lensing of the CMB anisotropy. When analyzing P18 data one discovers that  $A_L > 1$  is favored over  $A_L = 1$  at  $2.8\sigma$ , [19, 32, 46, 47]. We however note that a recent analysis of updated PR4 Planck data, [48], finds  $A_L > 1$  is favored over  $A_L = 1$  by only  $0.75\sigma$ . Another issue is that some SNIa data tend to favor higher values of  $\Omega_m$  than do other data. For example, in the flat  $\Lambda$ CDM model P18+lensing data give  $\Omega_m = 0.3153 \pm 0.0073$ , [32], while Pantheon+SNIa data give  $\Omega_m = 0.332 \pm 0.020$ , [34], which are not

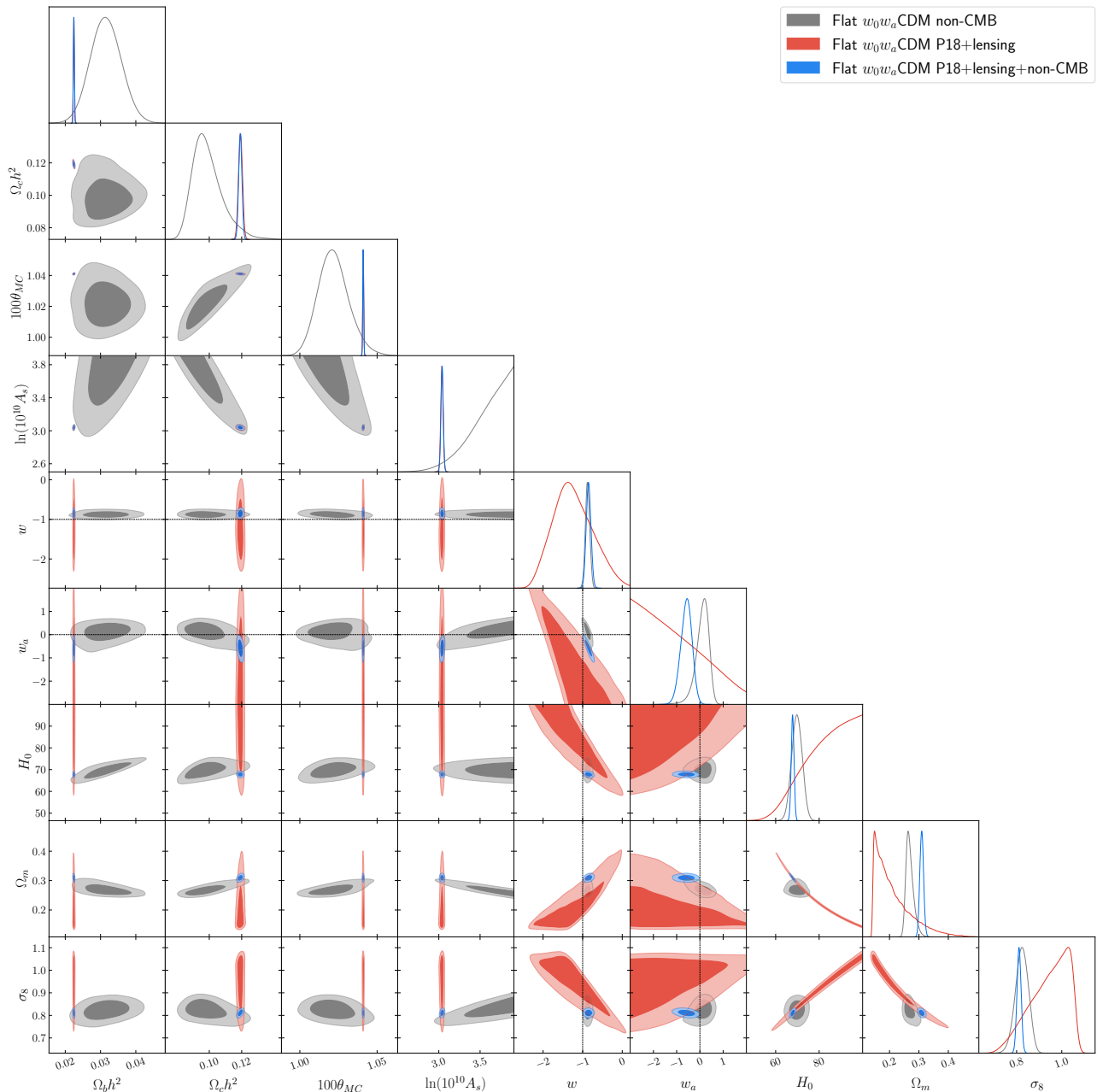


FIG. 2. One-dimensional likelihoods and  $1\sigma$  and  $2\sigma$  likelihood confidence contours of flat  $w_0w_a$ CDM model parameters favored by non-CMB, P18+lensing, P18+lensing+non-CMB data sets. We do not show  $\tau$  and  $n_s$ , which are fixed in the non-CMB data analysis.

that discrepant, but other SNIa data (which we do not use here) give higher values,  $\Omega_m = 0.356^{+0.028}_{-0.026}$ , [49], and  $\Omega_m = 0.352 \pm 0.017$ , [50]. So it is probably not inconceivable that there might be a few as yet undiscovered systematics in some cosmological data.

Comparing the flat  $\Lambda$ CDM model cosmological parameter values constrained by the P18+lensing+non-CMB (new) data, listed in the right column of the upper panel of Table IV of [19], to those for the same data but for the flat  $w_0w_a$ CDM model shown in the right column of Table

I here, we find that the six common primary parameter values are in good agreement, with the differences being  $0.26\sigma$  for  $\Omega_b h^2$ ,  $-0.47\sigma$  for  $\Omega_c h^2$ ,  $0.22\sigma$  for  $100\theta_{MC}$ ,  $0.35\sigma$  for  $\tau$ ,  $0.28\sigma$  for  $n_s$ , and  $0.30\sigma$  for  $\ln(10^{10}A_s)$ , with equally small derived-parameter differences of  $0.34\sigma$  for  $H_0$ ,  $-0.44\sigma$  for  $\Omega_m$ , and  $-0.29\sigma$  for  $\sigma_8$ . It is encouraging that current data compilations are able to provide almost cosmological-model-independent main cosmological parameter constraints.

From the P18+lensing+non-CMB data set in the flat

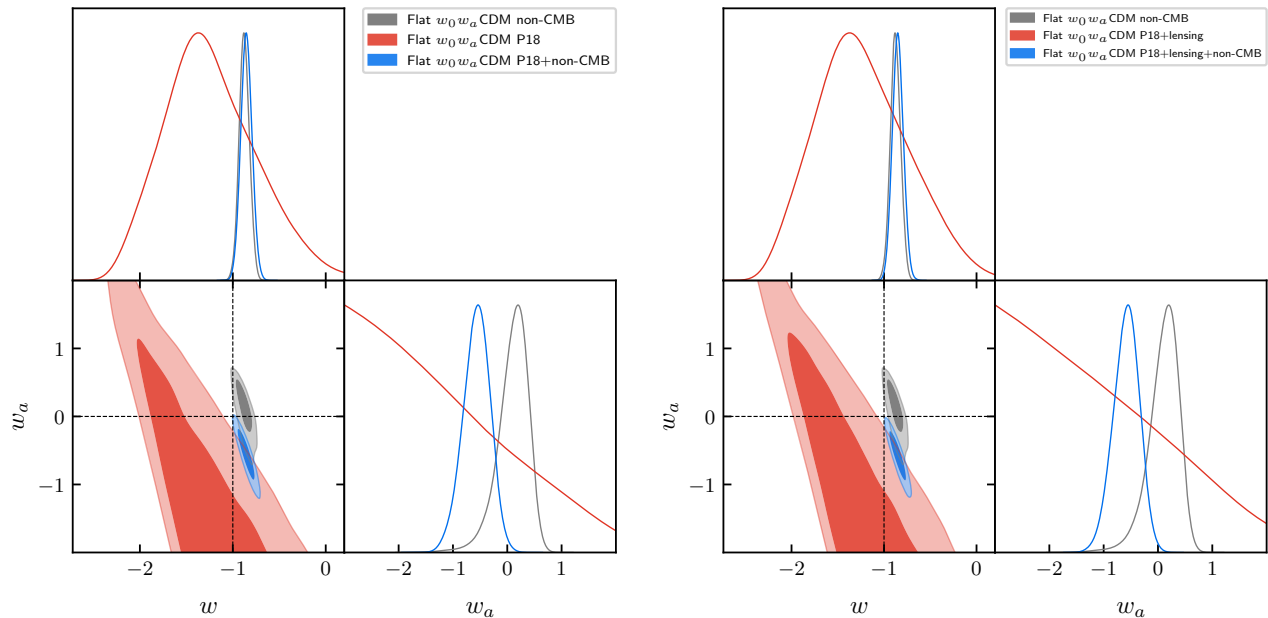


FIG. 3. One-dimensional likelihoods and  $1\sigma$  and  $2\sigma$  likelihood confidence contours of  $w_0$  and  $w_a$  parameters in the flat  $w_0 w_a$ CDM model favored by (left) non-CMB, P18, and P18+non-CMB data sets, and (right) non-CMB, P18+lensing, and P18+lensing+non-CMB data sets.

TABLE II. Consistency check parameter  $\log_{10} \mathcal{I}$  and tension parameters  $\sigma$  and  $p$  for P18 vs. non-CMB data sets and P18+lensing vs. non-CMB data sets in the flat  $w_0 w_a$ CDM model.

Data	P18 vs non-CMB	P18+lensing vs non-CMB
$\log_{10} \mathcal{I}$	-0.891	-0.787
$\sigma$	2.801	2.653
$p$ (%)	0.509	0.798

$w_0 w_a$ CDM model we get  $H_0 = 67.80 \pm 0.64$  km s $^{-1}$  Mpc $^{-1}$ , which agrees with the median statistics result  $H_0 = 68 \pm 2.8$  km s $^{-1}$  Mpc $^{-1}$  [51–53], as well as with some other local measurements including the flat  $\Lambda$ CDM model value of [34]  $H_0 = 69.5 \pm 2.4$  km s $^{-1}$  Mpc $^{-1}$  from a joint analysis of  $H(z)$ , BAO, Pantheon+ SNIa, quasar angular size, reverberation-measured Mg II and C IV quasar, and 118 Amati correlation gamma-ray burst data, and the local  $H_0 = 69.8 \pm 1.7$  km s $^{-1}$  Mpc $^{-1}$  from TRGB and SNIa data [54], but is in tension with the local  $H_0 = 73.04 \pm 1.04$  km s $^{-1}$  Mpc $^{-1}$  measured using Cepheids and SNIa data [55], also see [56]. And the flat  $w_0 w_a$ CDM model P18+lensing+non-CMB data value  $\Omega_m = 0.3094 \pm 0.0063$  also agrees well with the flat  $\Lambda$ CDM model value of  $\Omega_m = 0.313 \pm 0.012$  of [34] (for the data set listed above used to determine  $H_0$ ).

The DESI collaboration, [6], compile the DESI+CMB+PantheonPlus data set, from DESI 2024 BAO measurements (DESI), P18 power spec-

tra measurements [31, 32] combined with updated Planck and Atacama Cosmology Telescope lensing potential power spectrum measurements [57–59] (CMB), and Pantheon+ SNIa [33] (PantheonPlus). From the DESI+CMB+PantheonPlus data in the flat  $w_0 w_a$ CDM model they measure (and list in their Table 3)  $w_0 = -0.827 \pm 0.063$ ,  $w_a = -0.75^{+0.29}_{-0.25}$ ,  $H_0 = 68.03 \pm 0.72$  km s $^{-1}$  Mpc $^{-1}$ , and  $\Omega_m = 0.3085 \pm 0.0068$ , differing by  $-0.27\sigma$ ,  $0.44\sigma$ ,  $-0.24\sigma$ , and  $0.097\sigma$ , respectively from our somewhat more restrictive P18+lensing+non-CMB values of  $w_0 = -0.850 \pm 0.059$ ,  $w_a = -0.59^{+0.26}_{-0.22}$ ,  $H_0 = 67.80 \pm 0.64$  km s $^{-1}$  Mpc $^{-1}$ , and  $\Omega_m = 0.3094 \pm 0.0063$  listed in the right column of our Table I.

Comparing our  $w_0$ - $w_a$  likelihood contours of the flat  $w_0 w_a$ CDM model for the P18+lensing+non-CMB data, shown in the right panel of Fig. 3, to the corresponding DESI+CMB+PantheonPlus blue contours in the right panel of Fig. 6 of [6], we see that the upper left vertex of our  $2\sigma$  blue contour almost touches the flat  $\Lambda$ CDM model point of  $w = -1$  and  $w_a = 0$ , while the corresponding DESI+CMB+PantheonPlus point is slightly removed from the flat  $\Lambda$ CDM point towards slightly more negative values of  $w$  and  $w_a$ . The major axis of our  $2\sigma$  contour is roughly half as long as the corresponding DESI+CMB+PantheonPlus one, reflecting the greater constraining power of our data compilation.

From Table I we see that for P18+lensing+non-CMB data the flat  $w_0 w_a$ CDM model is positively favored over the flat  $\Lambda$ CDM model by  $\Delta\text{DIC} = -2.45$ , slightly more favored by these data than by

the DESI+CMB+PantheonPlus data compilation, where  $\Delta\text{DIC} = -2.0$ , [6], is on the borderline and indicates weak evidence for the flat  $w_0w_a\text{CDM}$  model.

## V. CONCLUSION

Using the P18+lensing+non-CMB data set of [19], that is about as independent of DESI 2024 data [6] as reasonably possible (there is some spatial overlap at lower  $z$  between some of the BAO data sets), we have confirmed the DESI 2024 finding that a dynamical dark energy density fluid parameterized by an evolving equation of state parameter  $w(z) = w_0 + w_a z/(1+z)$  with  $w_0 = -0.850 \pm 0.059$  and  $w_a = -0.59^{+0.26}_{-0.22}$ , is favored over a cosmological constant by  $\sim 2\sigma$ . Our P18+lensing+non-CMB data constraints on the flat  $w_0w_a\text{CDM}$  model cosmological parameters are slightly more restrictive than those derived from DESI+CMB+PantheonPlus data of [6]. P18+lensing+non-CMB data also slightly more strongly favor the flat  $w_0w_a\text{CDM}$  model over the flat  $\Lambda\text{CDM}$  model than do DESI+CMB+PantheonPlus data.

These are interesting results, not yet statistically significant, but certainly worth additional study. Importantly  $w(z) = w_0 + w_a z/(1+z)$  is a parameterization and not a physically consistent dynamical dark energy model. In the simplest physical dynamical dark energy models dark energy is modelled as a dynamical scalar field  $\phi$  with a self-interaction potential energy density  $V(\phi)$ , [20, 21]. For recent discussions of the DESI 2024 data constraints on dynamical scalar field dark energy models, see [22–24]. More importantly, of course, is the need for more data, which should soon be forthcoming from DESI.

## ACKNOWLEDGMENTS

J.d.C.P. was supported by the Margarita Salas fellowship funded by the European Union (NextGenerationEU). C.-G.P. was supported by a National Research Foundation of Korea (NRF) grant funded by the Korea government (MSIT) No. RS-2023-00246367.

- 
- [1] P. J. E. Peebles, Tests of Cosmological Models Constrained by Inflation, *Astrophys. J.* **284**, 439 (1984).
- [2] L. Perivolaropoulos and F. Skara, Challenges for  $\Lambda\text{CDM}$ : An update, *New Astron. Rev.* **95**, 101659 (2022), arXiv:2105.05208 [astro-ph.CO].
- [3] M. Moresco *et al.*, Unveiling the Universe with emerging cosmological probes, *Living Rev. Rel.* **25**, 6 (2022), arXiv:2201.07241 [astro-ph.CO].
- [4] E. Abdalla *et al.*, Cosmology intertwined: A review of the particle physics, astrophysics, and cosmology associated with the cosmological tensions and anomalies, *JHEAp* **34**, 49 (2022), arXiv:2203.06142 [astro-ph.CO].
- [5] J.-P. Hu and F.-Y. Wang, Hubble Tension: The Evidence of New Physics, *Universe* **9**, 94 (2023), arXiv:2302.05709 [astro-ph.CO].
- [6] A. G. Adame *et al.* (DESI), DESI 2024 VI: Cosmological Constraints from the Measurements of Baryon Acoustic Oscillations, (2024), arXiv:2404.03002 [astro-ph.CO].
- [7] M. Chevallier and D. Polarski, Accelerating universes with scaling dark matter, *Int. J. Mod. Phys. D* **10**, 213 (2001), arXiv:gr-qc/0009008.
- [8] E. V. Linder, Exploring the expansion history of the universe, *Phys. Rev. Lett.* **90**, 091301 (2003), arXiv:astro-ph/0208512.
- [9] J. Solà, A. Gómez-Valent, and J. de Cruz Pérez, Dynamical dark energy: scalar fields and running vacuum, *Mod. Phys. Lett. A* **32**, 1750054 (2017), arXiv:1610.08965 [astro-ph.CO].
- [10] J. Ooba, B. Ratra, and N. Sugiyama, Planck 2015 constraints on spatially-flat dynamical dark energy models, *Astrophys. Space Sci.* **364**, 176 (2019), arXiv:1802.05571 [astro-ph.CO].
- [11] C.-G. Park and B. Ratra, Observational constraints on the tilted spatially-flat and the untilted nonflat  $\phi\text{CDM}$  dynamical dark energy inflation models, *Astrophys. J.* **868**, 83 (2018), arXiv:1807.07421 [astro-ph.CO].
- [12] J. Solà Peracaula, A. Gómez-Valent, and J. de Cruz Pérez, Signs of Dynamical Dark Energy in Current Observations, *Phys. Dark Univ.* **25**, 100311 (2019), arXiv:1811.03505 [astro-ph.CO].
- [13] C.-G. Park and B. Ratra, Using SPT polarization, *Planck* 2015, and non-CMB data to constrain tilted spatially-flat and untilted nonflat  $\Lambda\text{CDM}$ ,  $\text{XCDM}$ , and  $\phi\text{CDM}$  dark energy inflation cosmologies, *Phys. Rev. D* **101**, 083508 (2020), arXiv:1908.08477 [astro-ph.CO].
- [14] S. Cao, J. Ryan, and B. Ratra, Cosmological constraints from H ii starburst galaxy apparent magnitude and other cosmological measurements, *Mon. Not. Roy. Astron. Soc.* **497**, 3191 (2020), arXiv:2005.12617 [astro-ph.CO].
- [15] N. Khadka and B. Ratra, Constraints on cosmological parameters from gamma-ray burst peak photon energy and bolometric fluence measurements and other data, *Mon. Not. Roy. Astron. Soc.* **499**, 391 (2020), arXiv:2007.13907 [astro-ph.CO].
- [16] S. Cao and B. Ratra, Using lower redshift, non-CMB, data to constrain the Hubble constant and other cosmological parameters, *Mon. Not. Roy. Astron. Soc.* **513**, 5686 (2022), arXiv:2203.10825 [astro-ph.CO].
- [17] F. Dong, C. Park, S. E. Hong, J. Kim, H. Seong Hwang, H. Park, and S. Appleby, Tomographic Alcock–Paczynski Test with Redshift-space Correlation Function: Evidence for the Dark Energy Equation-of-state Parameter  $w > -1$ , *Astrophys. J.* **953**, 98 (2023), arXiv:2305.00206 [astro-ph.CO].
- [18] M. Van Raamsdonk and C. Waddell, Possible hints of decreasing dark energy from supernova data, arXiv:2305.04946 [astro-ph.CO].
- [19] J. de Cruz Pérez, C.-G. Park, and B. Ratra, Updated observational constraints on spatially-flat and non-flat  $\Lambda\text{CDM}$  and  $\text{XCDM}$  cosmological models, (2024),

- arXiv:2404.19194 [astro-ph.CO].
- [20] P. J. E. Peebles and B. Ratra, Cosmology with a Time Variable Cosmological Constant, *Astrophys. J. Lett.* **325**, L17 (1988).
- [21] B. Ratra and P. J. E. Peebles, Cosmological Consequences of a Rolling Homogeneous Scalar Field, *Phys. Rev. D* **37**, 3406 (1988).
- [22] Y. Tada and T. Terada, Quintessential interpretation of the evolving dark energy in light of DESI, (2024), arXiv:2404.05722 [astro-ph.CO].
- [23] W. Yin, Cosmic Clues: DESI, Dark Energy, and the Cosmological Constant Problem, (2024), arXiv:2404.06444 [hep-ph].
- [24] K. V. Berghaus, J. A. Kable, and V. Miranda, Quantifying Scalar Field Dynamics with DESI 2024 Y1 BAO measurements, (2024), arXiv:2404.14341 [astro-ph.CO].
- [25] D. Wang, Constraining Cosmological Physics with DESI BAO Observations, (2024), arXiv:2404.06796 [astro-ph.CO].
- [26] O. Luongo and M. Muccino, Model independent cosmographic constraints from DESI 2024, (2024), arXiv:2404.07070 [astro-ph.CO].
- [27] M. Cortès and A. R. Liddle, Interpreting DESI's evidence for evolving dark energy, (2024), arXiv:2404.08056 [astro-ph.CO].
- [28] E. O. Colgáin, M. G. Dainotti, S. Capozziello, S. Pourojaghi, M. M. Sheikh-Jabbari, and D. Stojkovic, Does DESI 2024 Confirm  $\Lambda$ CDM?, (2024), arXiv:2404.08633 [astro-ph.CO].
- [29] D. Wang, The Self-Consistency of DESI Analysis and Comment on "Does DESI 2024 Confirm  $\Lambda$ CDM?", (2024), arXiv:2404.13833 [astro-ph.CO].
- [30] H. Wang and Y.-S. Piao, Dark energy in light of recent DESI BAO and Hubble tension, (2024), arXiv:2404.18579 [astro-ph.CO].
- [31] N. Aghanim *et al.* (Planck), Planck 2018 results. I. Overview and the cosmological legacy of Planck, *Astron. Astrophys.* **641**, A1 (2020), arXiv:1807.06205 [astro-ph.CO].
- [32] N. Aghanim *et al.* (Planck), Planck 2018 results. VI. Cosmological parameters, *Astron. Astrophys.* **641**, A6 (2020), [Erratum: *Astron. Astrophys.* 652, C4 (2021)], arXiv:1807.06209 [astro-ph.CO].
- [33] D. Brout *et al.*, The Pantheon+ Analysis: Cosmological Constraints, *Astrophys. J.* **938**, 110 (2022), arXiv:2202.04077 [astro-ph.CO].
- [34] S. Cao and B. Ratra,  $H_0=69.8\pm 1.3$  km s<sup>-1</sup> Mpc<sup>-1</sup>,  $\Omega_{m0}=0.288\pm 0.017$ , and other constraints from lower-redshift, non-CMB, expansion-rate data, *Phys. Rev. D* **107**, 103521 (2023), arXiv:2302.14203 [astro-ph.CO].
- [35] A. Challinor and A. Lasenby, Cosmic microwave background anisotropies in the CDM model: A Covariant and gauge invariant approach, *Astrophys. J.* **513**, 1 (1999), arXiv:astro-ph/9804301.
- [36] A. Lewis, A. Challinor, and A. Lasenby, Efficient computation of CMB anisotropies in closed FRW models, *Astrophys. J.* **538**, 473 (2000), arXiv:astro-ph/9911177.
- [37] A. Lewis and S. Bridle, Cosmological parameters from CMB and other data: A Monte Carlo approach, *Phys. Rev. D* **66**, 103511 (2002), arXiv:astro-ph/0205436.
- [38] A. Lewis, GetDist: a Python package for analysing Monte Carlo samples, arXiv:1910.13970 [astro-ph.IM].
- [39] F. Lucchin and S. Matarrese, Power Law Inflation, *Phys. Rev. D* **32**, 1316 (1985).
- [40] B. Ratra, Quantum Mechanics of Exponential Potential Inflation, *Phys. Rev. D* **40**, 3939 (1989).
- [41] B. Ratra, Inflation in an Exponential Potential Scalar Field Model, *Phys. Rev. D* **45**, 1913 (1992).
- [42] S. Joudaki *et al.*, CFHTLenS revisited: assessing concordance with Planck including astrophysical systematics, *Mon. Not. Roy. Astron. Soc.* **465**, 2033 (2017), arXiv:1601.05786 [astro-ph.CO].
- [43] W. Handley and P. Lemos, Quantifying dimensionality: Bayesian cosmological model complexities, *Phys. Rev. D* **100**, 023512 (2019), arXiv:1903.06682.
- [44] W. Handley and P. Lemos, Quantifying tensions in cosmological parameters: Interpreting the DES evidence ratio, *Phys. Rev. D* **100**, 043504 (2019), arXiv:1902.04029.
- [45] W. Handley, Curvature tension: evidence for a closed universe, *Phys. Rev. D* **103**, L041301 (2021), arXiv:arXiv:1908.09139 [astro-ph.CO].
- [46] E. Calabrese, A. Slosar, A. Melchiorri, G. F. Smoot, and O. Zahn, Cosmic Microwave Weak lensing data as a test for the dark universe, *Phys. Rev. D* **77**, 123531 (2008), arXiv:arXiv:0803.2309 [astro-ph].
- [47] J. de Cruz Pérez, C.-G. Park, and B. Ratra, Current data are consistent with flat spatial hypersurfaces in the  $\Lambda$ CDM cosmological model but favor more lensing than the model predicts, *Phys. Rev. D* **107**, 063522 (2023), arXiv:2211.04268 [astro-ph.CO].
- [48] M. Tristram *et al.*, Cosmological parameters derived from the final Planck data release (PR4), *Astron. Astrophys.* **682**, A37 (2024), arXiv:2309.10034 [astro-ph.CO].
- [49] D. Rubin *et al.*, Union Through UNITY: Cosmology with 2,000 SNe Using a Unified Bayesian Framework, (2023), arXiv:2311.12098 [astro-ph.CO].
- [50] T. M. C. Abbott *et al.* (DES), The Dark Energy Survey: Cosmology Results With  $\sim 1500$  New High-redshift Type Ia Supernovae Using The Full 5-year Dataset, (2024), arXiv:2401.02929 [astro-ph.CO].
- [51] G. Chen and B. Ratra, Median statistics and the Hubble constant, *Publ. Astron. Soc. Pac.* **123**, 1127 (2011), arXiv:1105.5206., arXiv:1105.5206 [astro-ph.CO].
- [52] J. R. Gott, III, M. S. Vogeley, S. Podariu, and B. Ratra, Median statistics,  $H(0)$ , and the accelerating universe, *Astrophys. J.* **549**, 1 (2001), arXiv:astro-ph/0006103.
- [53] E. Calabrese, M. Archidiacono, A. Melchiorri, and B. Ratra, The impact of a new median statistics  $H_0$  prior on the evidence for dark radiation, *Phys. Rev. D* **86**, 043520 (2012), arXiv:arXiv:1205.6753 [astro-ph.CO].
- [54] W. L. Freedman, Measurements of the Hubble Constant: Tensions in Perspective, *Astrophys. J.* **919**, 16 (2021), arXiv:2106.15656 [astro-ph.CO].
- [55] A. G. Riess *et al.*, A Comprehensive Measurement of the Local Value of the Hubble Constant with 1 km/s/Mpc Uncertainty from the Hubble Space Telescope and the SH0ES Team, *Astrophys. J. Lett.* **934**, L7 (2022), arXiv:2112.04510 [astro-ph.CO].
- [56] Y. Chen, S. Kumar, B. Ratra, and T. Xu, Effects of Type Ia Supernovae Absolute Magnitude Priors on the Hubble Constant Value, *Astrophys. J. Lett.* **964**, L4 (2024), arXiv:2401.13187 [astro-ph.CO].
- [57] M. S. Madhavacheril *et al.* (ACT), The Atacama Cosmology Telescope: DR6 Gravitational Lensing Map and Cosmological Parameters, *Astrophys. J.* **962**, 113 (2024), arXiv:2304.05203 [astro-ph.CO].
- [58] F. J. Qu *et al.* (ACT), The Atacama Cosmology Telescope: A Measurement of the DR6 CMB Lensing Power

Spectrum and Its Implications for Structure Growth, *Astrophys. J.* **962**, 112 (2024), arXiv:2304.05202 [astro-ph.CO].

[59] N. MacCrann *et al.* (ACT), The Atacama Cosmology Telescope: Mitigating the impact of extragalactic fore-

grounds for the DR6 CMB lensing analysis, (2023), arXiv:2304.05196 [astro-ph.CO].